ARMA 12-189

SAND2012-1471C

Structural Integrity of Oil Storage Caverns at a Strategic Petroleum Reserve Site with Highly Heterogeneous Salt and Caprock

Sobolik, S.R. and Ehgartner, B.L.

Sandia National Laboratories, Albuquerque, New Mexico, USA

This paper was prepared for presentation at the 46th US Rock Mechanics / Geomechanics Symposium held in Chicago, IL, USA, 24-27 June 2012.

ABSTRACT: This paper presents computational analyses to evaluate the effects of heterogeneous salt creep properties, compromised caprock mined for sulfur, and pressure loss in an abandoned brine storage cavern, on cavern wellbore and surface structures at an underground oil storage facility. These analyses represent a first attempt to combine several complex, non-homogeneous processes in a dome-scale, three-dimensional geomechanical analysis using caverns meshed to measured geometries. The salt dome is characterized by heterogeneous salt properties, and nonuniformly-damaged caprock due to sulfur mining. Separate computational analyses in this report model the weakened caprock and identify a priority list for cavern borehole inspections, attempt to develop a set of salt creep properties from which predicted cavern volume closure matches measured values for individual caverns, and evaluate what effect that a damaged abandoned cavern may have on nearby caverns and their boreholes.

1. INTRODUCTION

The U.S. Strategic Petroleum Reserve (SPR), operated by the U.S. Department of Energy (DOE), stores crude oil in 62 caverns located at four different sites in Texas (Bryan Mound and Big Hill) and Louisiana (Bayou Choctaw and West Hackberry). The petroleum is stored in solution-mined caverns in salt dome formations. The Bryan Mound salt dome, located approximately 100 km south of Houston, Texas, near the city of Freeport, is the largest of the SPR sites in terms of oil-storage capacity (currently 43×10^6 m^3, or 226×10^6 barrels), and has operated since 1980. The geomechanical behavior of the site is characterized by two significant factors. One, the salt is bisected by several boundary shear zones consisting of faults, salt spines, and other anomalies. Due to these features, the salt creep rates are highly heterogeneous across the site, as measured by cavern closures that vary significantly throughout the salt dome. Two, sulfur mining in the caprock at Bryan Mound occurred in the early 20th century. Sulfur mining was performed using the Frasch extraction method, for which superheated steam at 160°C was injected into the caprock to draw out sulfur, in a mostly molten form with some SO_2 and H_2SO_4. This mining method both weakens the in situ rock and removes material, and thus induces underground collapse and subsidence; in the case of Bryan Mound, evidence of this subsidence is indirect, with no known monitoring program. The sulfur mining process also left a significant amount of heat in the caprock and upper dome that still remains. There is an additional cavern at Bryan Mound, Cavern 3, which was constructed for brine storage in the 1940s and plugged and abandoned in 1980. Surface subsidence measurements indicate that this cavern may have lost pressure, which would affect boreholes for nearby caverns. These factors introduce mechanical, thermal, and chemical environments that affect the long-term integrity of boreholes in the caprock and upper dome, and in fact several boreholes have been found to have suffered significant damage in the past few years.

This paper presents computational analyses to evaluate the effects of heterogeneous salt creep properties, compromised caprock mined for sulfur, and pressure loss in Cavern 3, on cavern wellbore and surface structures at an underground oil storage facility. These analyses represent a first attempt to combine several complex, non-homogeneous processes in a dome-scale, three-dimensional geomechanical analysis using caverns meshed to measured geometries. The first set of calculations modeled a weakened caprock and identified a priority list for cavern borehole inspections. Additional computational analyses developed a set of salt creep properties from which predicted cavern volume closure provided improved matches with measured values for individual caverns. Finally, the improved model was used to evaluate what effect that a damaged Cavern 3 may have on nearby caverns and their boreholes.

2. SITE DESCRIPTION

The geological characteristics related to the Bryan Mound site have been progressively described with

greater detail [1-5]. The Bryan Mound caverns have been extensively characterized and mapped in a sonar atlas prepared [5, 6].

Figures 1 and 2 show plan views of the Bryan Mound site with the caverns' approximate locations within the salt dome, and the interface of the salt dome with the caprock and surrounding sandstone. Caverns 1 through 5 (also referred to as the Phase 1 caverns) were initially developed by Dow in 1942 for brine production in the period 1942 to 1957. These five caverns have very irregular shapes. Four of these caverns (Caverns 1, 2, 4 and 5) were purchased for the SPR in 1977 and certified as suitable for oil storage. Cavern 3 was shut down in 1957 due to its large roof span. Caverns 101-116 (Phase 2 caverns) were constructed by solution mining between 1981 and 1984 for oil storage, and have the more typical tapered cylindrical shape. An updated geologic perspective of the salt dome and caprock are provided in Figure 3[6]. Note that there seem to be two regions within the salt dome that are possibly separated by a salt spine or shear zone. The thickest caprock regions correspond to the two separate regions inferred from the structure contour map. Further study of the sonar data used to characterize the salt dome reveal the orientation of potential boundary shear zones within the salt dome; these zones are shown in Figure 4 [6]. Of the three boundary shear zones shown in Figure 3, the one of greatest interest is that which is in the southeast portion of the salt dome, running roughly southwest to northeast. Caverns 106, 109, 112, 113, and 114 are located to the south of this shear zone. This region of the salt dome appears to contain salt with creep properties leading to higher creep rates than the remainder of the dome. Cavern 3 can be seen in Figure 4 as the largest cavern at the western edge of the dome.

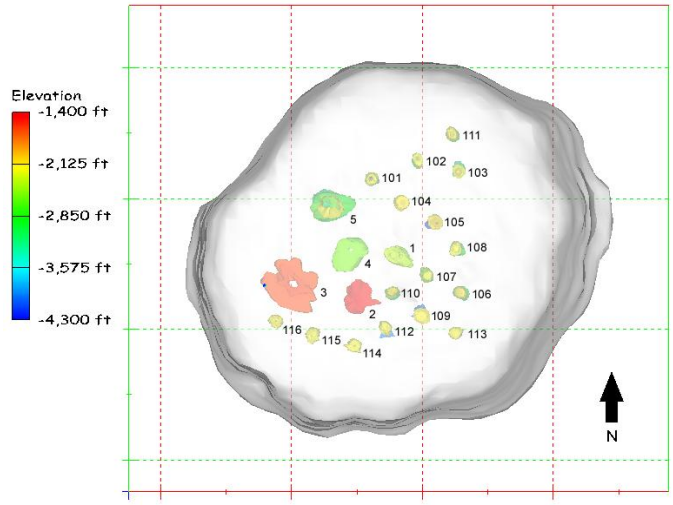

Fig. 1. Top view of the Bryan Mound salt dome and oil storage cavern model (610 m grid spacing).

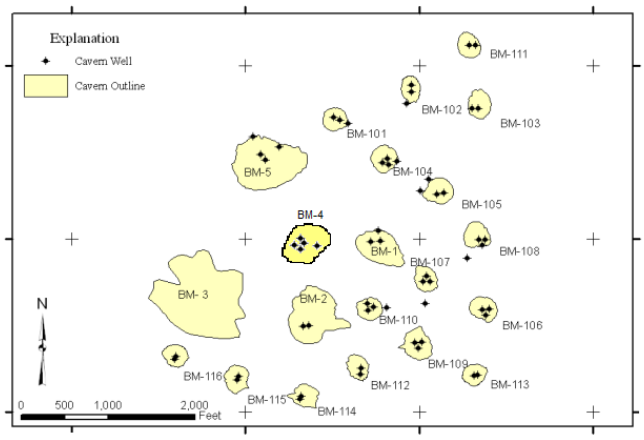

Fig. 2. Schematic of the Location of the SPR Caverns at Bryan Mound.

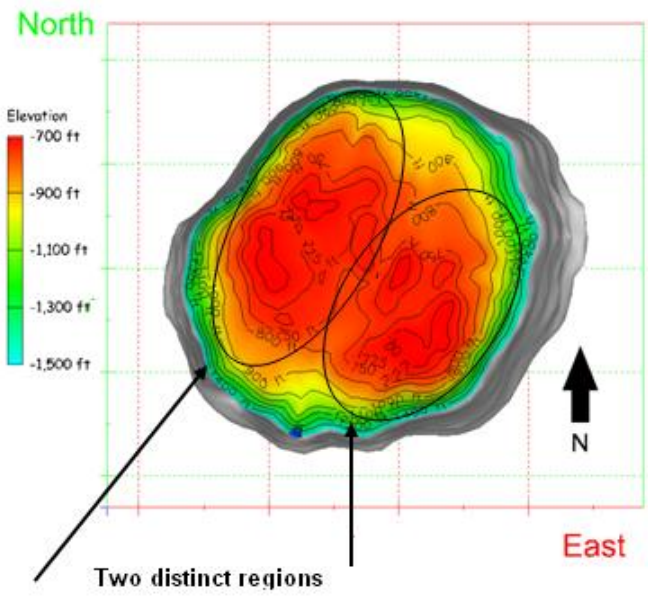

Fig. 3. 3-D model of the top of caprock and top of salt); contours are caprock thickness in feet [6].

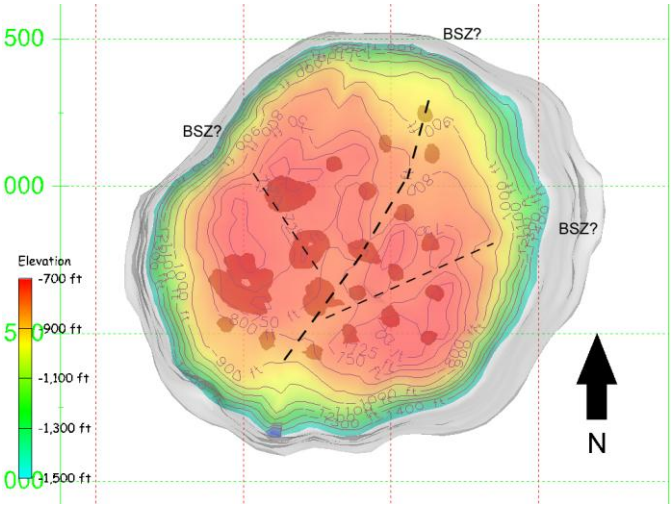

Fig. 4. Potential boundary shear zones in the Bryan Mound salt dome [6].

Figure 5 shows the oil storage cavern geometries based on sonar measurements obtained through 2007 [5, 6]. Note the enlarged tops and asymmetries of the cavern shapes. In general, caverns in the SPR are intentionally shaped with larger tops to accommodate future oil drawdowns where only the bottom portions of the caverns are preferentially leached, and hence the overall cavern shape becomes more cylindrical, due to raw water injections to remove the oil. Salt properties also result in unpredictable cavern shapes as the insoluble content or dissolution rates of salt can spatially vary. This explains some of the asymmetries found in the cavern shapes.

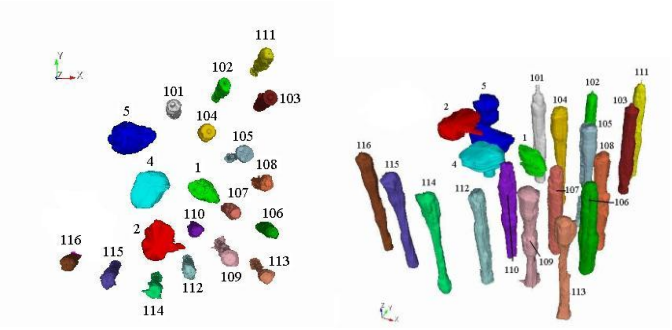

Fig. 5. Visualization of the caverns at Bryan Mound SPR site.

There exist three distinguishing features at the Bryan Mound that affect site operations and the structural integrity of surface and underground structures. The features include heterogeneous salt creep properties, due to faulting, boundary shear zones, and varying levels of anhydrite impurities throughout the salt dome; a caprock was mined for sulfur in the early 20th century, resulting in significant regions of caprock that are structurally compromised and a residual high temperature environment; and potential pressure loss in the abandoned brine storage Cavern 3. These features also affect the ability to use site data and computational analysis to evaluate the geomechanical processes important to structural stability of the caverns, wellbores, and surface facilities.

2.1. Heterogeneous Salt

The nonhomogeneous conditions of the salt described above – boundary shear zones, faults, varying impurity content – result in highly heterogeneous salt properties throughout the salt dome. These heterogeneous properties are expressed by the amount of volume loss due to creep that is experienced by the caverns throughout the site. There is a noticeably higher creep closure experienced by cavern to the south of the primary boundary shear layer. However, the more general case is that creep properties are irregular across the site. Table 1 lists the measure volume closure rates during normal operating pressures for the Phase 2 caverns in barrels per year (BBL/year). These caverns are all of similar shape and size, ranging from 1.4-1.9×10^6 m^3 (9-12×10^6 barrels). For a more homogeneous salt, these values should have a much smaller range. For Bryan Mound, both the range and spatial variability of the values make it difficult to develop model parameters that produce predicted behaviors that sufficiently match those observed in the field. The ability to produce a verifiable model is important for prediction of stress environment that are potentially detrimental to surface and subsurface facilities.

Table 1. Measured cavern closure rates under normal operating pressures in BBL/year for Bryan Mound Phase 2 caverns.

Cavern	Closure, BBL/yr	Cavern	Closure, BBL/yr
BM101	5,365	BM109	8,543
BM102	4,944	BM110	3,150
BM103	11,680	BM111	7,813
BM104	2,948	BM112	6,858
BM105	3,683	BM113	10,223
BM106	10,460	BM114	21,304
BM107	4,061	BM115	21,034
BM108	2,702	BM116	6,135

2.2. Sulfur Mining in the Caprock

Sulfur mining in the caprock at Bryan Mound began in the early 20th century. Sulfur mining operations began in 1914, and during the period 1914-1925 at least 0.6 m of subsidence had occurred (although there is no documented mention of where or how that was measured). The mining was performed using the Frasch Extraction Method, for which steam was injected into the caprock to draw out sulfur in the form of SO_2 and H_2SO_4. This mining method induces underground collapse and subsidence; in the case of Bryan Mound, evidence of this subsidence is indirect, with no known monitoring program.

The most relevant information from all these reports on sulfur mining at Bryan Mound is that approximately five million log tons of sulfur were removed from the caprock directly over the salt dome. That amount translates to an average of approximately one cubic meter of sulfur mined per square meter of area over the dome. The average thickness of the caprock is approximately 85 meters, so the removed sulfur represents about 1% of the thickness of the caprock. The void space created by the excavated sulfur may be in the form of new or enlarged pores, similar but larger vugs, or in new or expanded fractures. The creation of additional fracture space could result in a reduced rock mass bulk modulus. Also, the sulfur was not removed uniformly throughout the caprock. Figure 6 maps the locations of the sulfur mining wells; the large majority of these well occur around the rim of the dome, although significant numbers are scattered throughout the middle of the dome near the current SPR caverns as well. A non-uniform damage pattern in the caprock may affect the location of high stresses and strains.

Fig. 6. Structure of the Bryan Mound dome featuring locations of sulfur mining wells.

Because of the steam injection mining technique used at Bryan Mound, high residual temperatures occur throughout the caprock and conducted into the underlying salt dome. Borehole temperature logs were taken for each cavern between 2001 and 2003. These vertical temperature profiles are plotted in Figure 7. The caverns with the lowest maximum temperatures, Caverns 111, 114, 115, and 116, all lie on the periphery of the cavern field. The red linear plot in Figure 7 represents an in situ profile based on an independent borehole temperature log in salt at cavern depth; this linear profile has been used in the past for modeling exercises. However, a curve fit based on the average measured temperatures was used for this analysis; this curve fit is also shown in Figure 7.

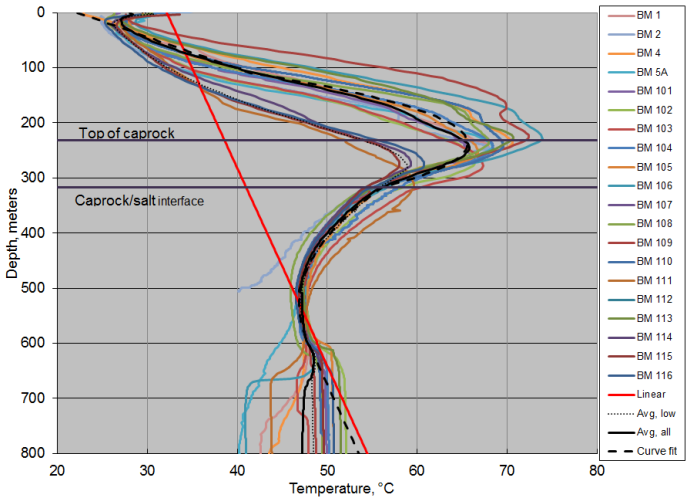

Fig. 7. Temperature profiles (2001-2003), including measurements from each borehole, average values and curve fits.

2.3. Abandoned Cavern 3

Cavern 3, located in the southwestern quadrant of the dome (Figures 4 and 5), contained a volume of 1.02×10^6 m^3 (6.4 MMB) based upon a 1979 sonar survey. The roof is highly irregular and the maximum diameter of the cavern (~410 m) is the largest of any of the DOE owned caverns. About two years after it was shut down, the pressure dropped. Testing by Dow showed the well had hydraulic integrity, but not the cavern. The original 213 mm (8.375 inch) production casing failed in the mid-1950s, and a 140 mm (5.5 inch) casing was cemented in. Dow believed the cavern was in communication with the top of salt. A number of tests fluid level and brine sampling tests and cased hole logs were performed in Cavern 3 in 1977. The cavern was not certified and the test results were not formally reported as were the results from the other caverns which were certified [1, 7]. Brine samples taken at three different times between November 1977 and April 1978 showed significant variations in composition suggesting that circulation was occurring in the cavern. Later tests performed for SPR [7] to determine fresh water circulation within the cavern were inconclusive, but the fact remained that the cavern did not hold pressure and therefore was not recommended for oil storage. Two computational analyses of Cavern 3 [1, 2] both concluded that Cavern 3 was structurally stable, and neither study predicted tensile stresses in the roof of the cavern. Neither study indicated that Cavern 3 was hydraulically stable, and both studies agreed with the recommendation that Cavern 3 should not be used for oil storage. Additionally, three surveys of the wells at Cavern 3 noted the presence of a void in the caprock of several feet in height at around 818 feet depth, and the height of the void decreased in succeeding reports [7 included the latest of these surveys]. This void in the caprock has been assumed to have resulted from the sulfur mining at Bryan Mound.

Recently, erratic surface subsidence measurements in the vicinity of Cavern 3 have been observed [8, 9]. Figure 8 plots the measured subsidence rates over the Bryan Mound site based on the site-wide measurements taken in January 2007 and April 2009. Figure 9 plots the subsidence rates over the site based on site-wide measurements taken in April 2009 and October 2010 [9]. Both figures indicate an increase in subsidence rate over Cavern 3 as compared to the rest of the Bryan Mound site, although the later plot shows a smaller difference. After the 2009 subsidence report [8], 15 new monuments were installed at Bryan Mound, with five over Cavern 3. While there have been no signs of damage resulting from this increase in subsidence activity over Cavern 3, longstanding concerns of the effects of the cavern on the stability of surrounding caverns have been increased.

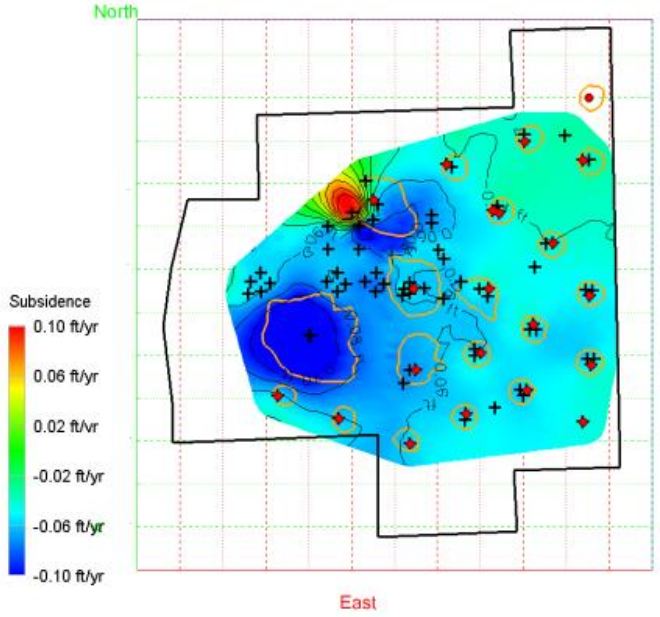

Fig. 8. Contour plot of subsidence rates (ft/yr) from January 2007 to April 2009.

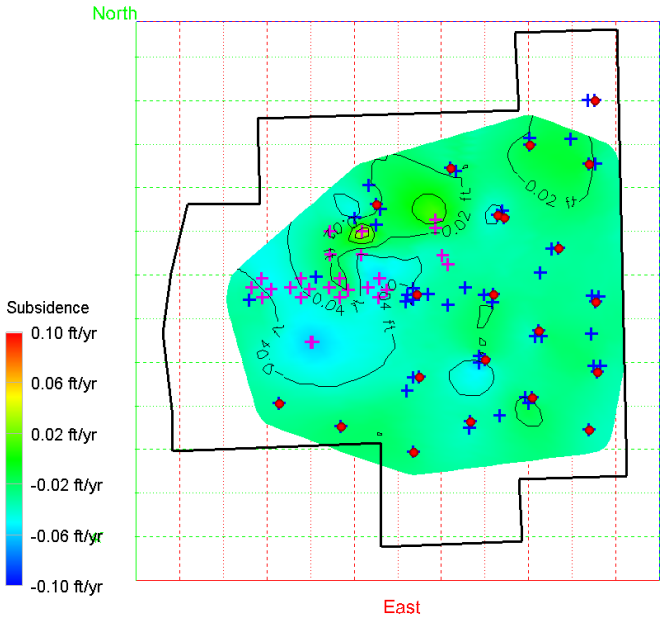

Fig. 9. Contour plot of subsidence rates (ft/yr) from April 2009 to Oct. 2010.

3. ANALYSES

Previous analyses of the Bryan Mound site have been performed to evaluate the evolving stress field at the site and its effect on surface and subsurface facilities [10]. These analyses included three-dimensional renderings of the salt dome and caverns to realistic geometries as measured by sonars, and several assumptions of the geomechanical behavior of the geologic media at the site, including:

- Salt creep properties based on values obtained from laboratory measurements [11], at further modified based on site measurements of subsidence and cavern closure. The analyses in [10] assumed a hard and soft section of salt, divided by the primary boundary shear zone in the southern part of the dome;
- An intact caprock that behaved elastically,

Those analyses have been useful toward understanding the processes at Bryan Mound, but their results still had significant discrepancies with observed behavior at the site. There were significant differences between predicted and measured subsidence and cavern closure behaviors; modeling the dome as two sections, hard and soft, provided better agreement than as a single dome, but the discrepancies were still larger than deemed acceptable. Also, those analyses predicted elongation along the boreholes casings and liners that resulted in axial strains in the caprock section not exceeding the prescribed threshold strains for cement and steel casings. These analytical results came into question when several well casings at Bryan Mound developed damage of various types; an example is shown in Figure 10. None of the documented damage appeared to be a joint separation due to excessive elongation, which would have been the type most expected. Instead, the damage appears to be one of several varieties: outward bowing of the walls of the casing due to axial compression; intrusion of cement or steel into the wellbore; or shear damage due to horizontal shear or twisting stresses. These incidents made it obvious that the caprock in which these casings are installed was not behaving as previously modeled, and that unusual stresses are being generated at the casings. In addition, higher temperatures and acidic environments left over from the sulfur mining of the early 1900s may enhance the mechanical and corrosive environments in the caprock. The recent discovery of increased subsidence over Cavern 3 provided additional concerns for structural stability.

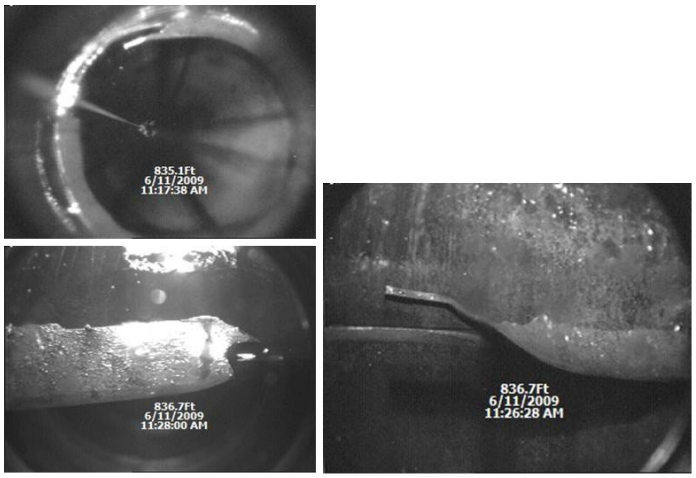

Fig. 10. Pictures of well damage at Bryan Mound well 106B.

As a result, several analyses have been performed over the past two years to evaluate different mechanical behaviors in the caprock, develop an improved suite of creep properties for the site, and evaluate the potential

impact of increased pressure loss form Cavern 3. These analyses, and the numerical models implemented for them, are described below.

3.1. Numerical and Material Models

These analyses utilized JAS3D, Version 2.0.F [12], a three-dimensional finite element program developed by Sandia National Laboratories, and designed to solve large quasi-static nonlinear mechanics problems. Several constitutive material models are incorporated into the program, including models that account for elasticity, viscoelasticity, several types of hardening plasticity, strain rate dependent behavior, damage, creep, and incompressibility. The continuum mechanics modeled by JAS3D are based on two fundamental governing equations. The kinematics are based on the conservation of momentum equation, which can be solved either for quasi-static or dynamic conditions (a quasi-static procedure was used for these analyses). The stress-strain relationships are posed in terms of the conventional Cauchy stress.

The power law creep model has been used for Waste Isolation Pilot Plan (WIPP) and SPR simulations for many years. This creep constitutive model considered only secondary or steady-state creep. The creep steady state strain rate is determined from the effective stress as follows:

$$\dot{\varepsilon} = A(\sigma)^n \exp\left(-\frac{Q}{RT}\right), \qquad (1)$$

where, $\dot{\varepsilon}$ = creep strain rate,
σ = effective or von Mises stress,
T = absolute temperature**,**
A, n = constants determined from fitting the model to creep data,
Q = effective activation energy,
R = universal gas constant.

The property set for Bryan Mound salt from [11] is listed in Table 2. A creep coefficient calibration was attempted by [10] for the soft and hard salts of the Bryan Mound salt dome. That analysis used the properties in Table 2, and increased the creep constant A for the hard and soft salts by factors of 1.8 and 13, respectively. As part of the implementation of the power law creep model, an elastic modulus reduction factor (RF) was used to simulate the immediate primary creep response that is not captured in the power law creep (i.e. secondary creep) model. In order to obtain agreement with the measured closure of underground drifts at the WIPP, a reduced modulus was initially used to simulate the transient response of salt [13]. Limited creep testing of SPR salts [14] showed considerable variability in creep rates (up to an order of magnitude difference). For these analyses, the modulus values in Table 2 are obtained from the standard modulus values in [11] divided by a reduction factor of 12.5.

Table 2. Power law creep mechanical properties for Bryan Mound salt.

Baseline Property from [11]	
Density, kg/m^3	2300
Elastic modulus, MPa	3100
Bulk modulus, MPa	2070
Poisson's ratio	0.25
Creep Constant A, 1/(Pa ^{n}-sec)	5.69×10^{-39}
Exponent n	5.0
Q, cal/mol	10000
Thermal constant Q/R, K	5033

The surface overburden layer, which mostly comprises sand and sandstone, and the sandstone surrounding the salt dome are considered isotropic and elastic, and have no assumed failure criteria. The caprock layer, consisting of anhydrite and limestone with some gypsum, is usually assumed to be elastic; some of the calculations in this paper maintain this assumption. Mechanical properties of each of these geologic materials used in the present analysis are listed in Table 3.

Table 3. Material properties of other geologic materials.

Parameters	Units	Overburden	Caprock	Sandstone
Density	kg/m^3	1870.	2500	2140
Elastic modulus	MPa	100	7000	7300
Poisson's ratio		0.33	0.29	0.33

For all the calculations included in this paper, the entire lives of the caverns (construction, brine or oil storage, operating and workover pressures) are modeled individually for each cavern. The modeled caverns are maintained at constant operating pressures except during workovers. The standard pressure condition applied to the cavern is based on an average wellhead pressure ranging between 6.20 and 6.72 MPa (900-975 psi). Beginning in the simulation year 1984, a series of five-year cycles of cavern workovers was initiated, during which every cavern is scheduled for a workover. During the workover, the affected cavern is held at 0 psi wellhead pressure for three months.

3.2. Damaged Caprock Model

The caprock at Bryan Mound affects stresses, strains, and damage modes of the wellbore casings by the following parameters:

- Caprock is naturally an inelastic medium, and requires a model that allows inelastic behavior such as crushing of void space in the rock;
- The caprock was mechanically weakened due to the removal of sulfur by fracturing and steam injection;

- The temperatures in sections of the caprock are 15C-20C higher than the ambient temperature at the same depth, causing both thermal expansion effects on stress and a heightened corrosive environment; and
- The sulfur mining process using steam injection also left a higher acidic environment, which could enhance corrosion.

In several previous analyses, SPR sites have been modeled using a 30-degree wedge section cut out of a 19-cavern field. This approach can allow for several sets of calculations to be performed, varying only certain parameters, to allow for a sort of parametric study. The mesh for the computational model is illustrated in Figure 11. The 30-degree wedge format with four caverns, a cylindrical salt dome and caprock, and vertical planes of symmetry was designed to simulate a storage facility with 19 caverns. Cavern 1 represents one cavern at the center of the 19-cavern field, and caverns 2, 3, and 4 each represent 6 caverns in the field due to model symmetry. The model is described in greater detail in [15].

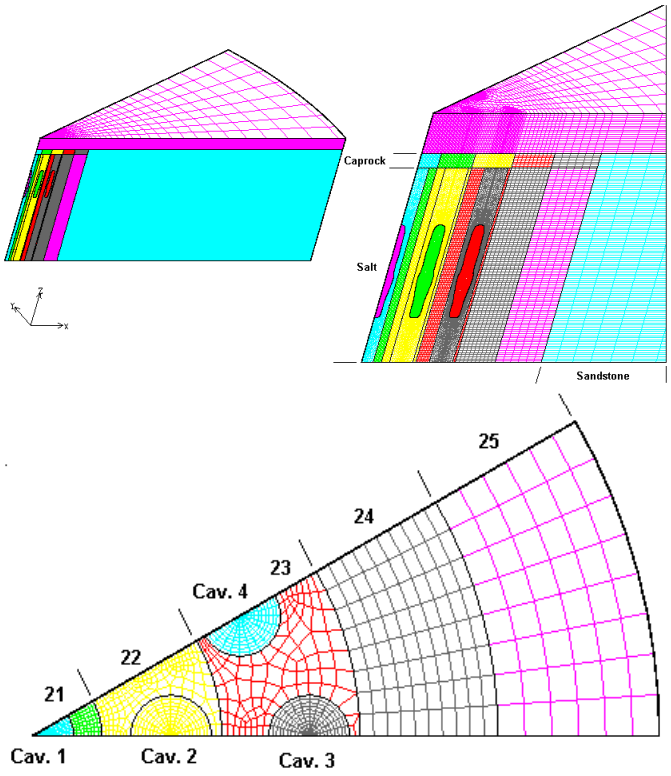

Fig. 11. Views of the computational mesh used for the damaged caprock calculations.

Figure 11 shows that the caprock was divided into 5 sections (with material numbers 21 through 25), and the locations of the caverns within these sections. An examination of the locations of sulfur mining wells in Figure 6 indicates that the largest percentage of the wells were located near the outer circumference of the salt dome. Other wells were interspersed throughout the dome, with some wells located above existing caverns and some clustered between caverns. The non-uniformity of the locations of mining wells suggests that mining-induced damage to the caprock in also non-uniform and may cause bending moments or shear regions within the caprock. Such conditions would put unusual stress and strain conditions on the well casings, and if large enough, may produce damage conditions. Therefore, the computational mesh was designed to allow for regional variations in mechanical properties in the caprock, based on where mining was more prominent.

Earlier Bryan Mound analyses treated the caprock as an elastic medium. For these calculations, it was assumed that the caprock does not necessarily behave elastically under normal circumstances, and that sulfur mining operations caused further damage to the caprock, thus changing its mechanical behavior. A series of sensitivity calculations were performed, alternating the use of an elastic model or a soil and foams model for the caprock; the latter model is for crushable, porous material that is often used for rock when properties are available from laboratory tests. No information on mechanical properties for the Bryan Mound caprock was available, so cited properties for caprock at another SPR site were used [16]. In addition, different methods were implemented to approximate the damage to the caprock caused by sulfur mining. Three methods were used: 1) altering one of the coefficients in the soil model to simulate a more porous, crushable rock; 2) reducing the Young's modulus by a factor of 10, to account for the creation of fractures and removal of material by mining (this estimate is a standard practice in other mining applications); and 3) altering the creep coefficient of the salt between hard and soft values. Furthermore, some calculations utilized the same properties for the entire caprock, and others applied damaged properties to alternating segments of the caprock (either to sections 21, 23, and 25, or to sections 22 and 24, and shown in Figure 11).

The physical presence of well casings are not included in this model, but the potential for ground deformation to damage these structures can be conservatively estimated by assuming that they will deform according to the predicted stresses and strains in the host rock. Several casing damage thresholds were calculated for the casings at Bryan Mound [15], and these were used to quantify potential damage scenarios:

- Axial strain of steel casing – 1.6 millistrains;
- Axial strain of cement liners – 0.2 millistrains;
- Collapse pressure of steel casing from maximum normal stress – 4.8 MPa (100 kpsf) warning stress for unpressurized casing, 9.6 MPa (200 kpsf) as threshold stress for collapse;
- Shear stress of caprock near borehole – 241 MPa (5.04 Mpsf) for steel, 17 MPa (360 kpsf) for cement;
- Combination of high values of any of these criteria.

3.3. *Cavern-Specific Creep Model*

The mesh developed for the computational model of the entire Bryan Mound salt dome is illustrated in Figures 12 and 13. Figure 12 shows the entire mesh used for these calculations, and Figure 13 shows the same view with the overburden and surrounding rock removed to expose the caprock and salt formations. The overburden and caprock thicknesses are reasonably constant over the entire salt dome, so for meshing purposes they have been given constant values; the overburden layer is 232 m thick, and the caprock 85 m thick. Figure 14 shows a plan view of the meshed caverns used for these calculations showing their placement within the salt dome.

Because of the highly nonhomogeneous nature of the salt at Bryan Mound, the properties listed in Table 2 provided predictions of cavern closure and surface subsidence that matched measured data with only mixed success [10]. The complexity of the non-homogeneity of the salt make the development of a strictly data-based creep property set impractical. To obtain better agreement between predictions and measurements, it was decided to develop a set of cavern-specific creep properties. Individual creep properties were assigned to the cylinder surrounding each cavern in the computational mesh, as shown in Figure 10. Several versions were run until a set was obtained for these analyses that provide significantly better correlation to measured values of cavern closure and surface subsidence than did the earlier analysis [10]. The details of this model are more completely described in [17].

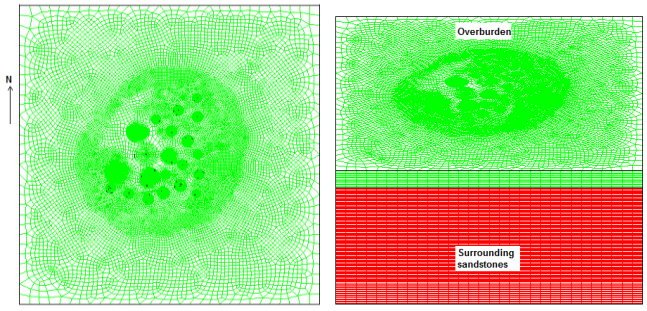

Fig. 12. Computational mesh developed for the Bryan Mound calculations.

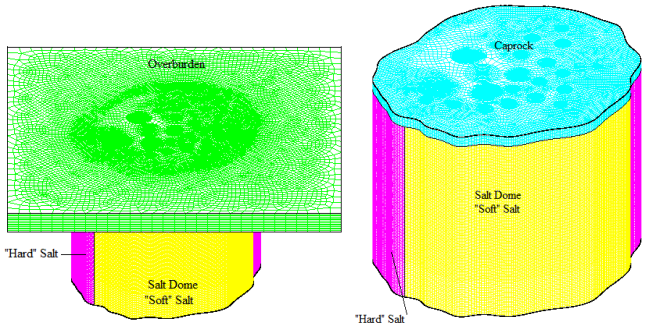

Fig. 13. Views of the computational mesh used for the damaged caprock calculations.

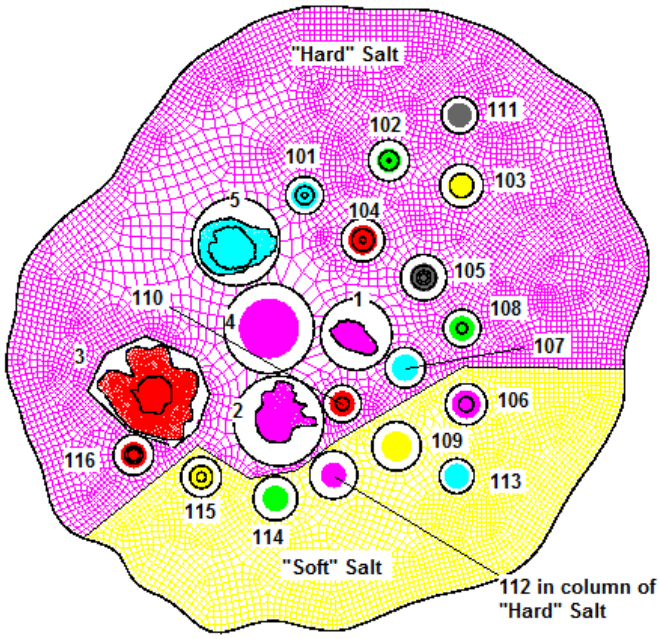

Fig. 14. Bryan Mound caverns in the computational mesh.

3.4. *Cavern 3 Model*

Several sets of quarterly elevation data were obtained from the new monuments installed over Cavern 3 in early 2010. Figure 15 shows the subsidence rates calculated between each set of site-wide elevation data taken for a location near Well 3, an average for all the cavern wells, and an average for all the stations at Bryan Mound. Figure 15 also contains a single point representing the subsidence rate measured from the new monuments between May 2010 and July 2011, with a subsidence rate of 20 mm/yr (0.069 ft/yr). The general trend over the years is for the subsidence rate to decrease, as would be expected. However, after 2003, the subsidence rate over Cavern 3 increases significantly. In [10], it was unclear whether this increase was real because of data collection problems outlined therein. However, data from the new monuments indicate that the increased subsidence rate over Cavern 3 is real. It is not clear from the data whether the increased subsidence over Cavern 3 has had an effect on subsidence over the entire site.

After the calculations to develop cavern-specific creep properties had been completed, additional calculations were performed to determine the effect of cavern 3 on the stresses in the surrounding salt dome and surface. An initial set of calculations indicated that, if it has been properly sealed and is behaving normally, the presence of Cavern 3 should have a negligible effect on subsidence, as well as the geomechanical stresses and strains in the area. This lack of an effect is largely because the cavern pressure is not being cycled due to workovers, as is necessary in the oil storage caverns, so there are no changes in the stress around the cavern that cause an increased creep rate. The cavern's location

high in the salt dome, where there is a smaller difference between cavern fluid pressure and in situ pressure than at greater depths, also diminished the effect of Cavern 3. There are higher temperatures at that location from sulfur mining, which enhance creep, but the smaller pressure differential diminishes that response.

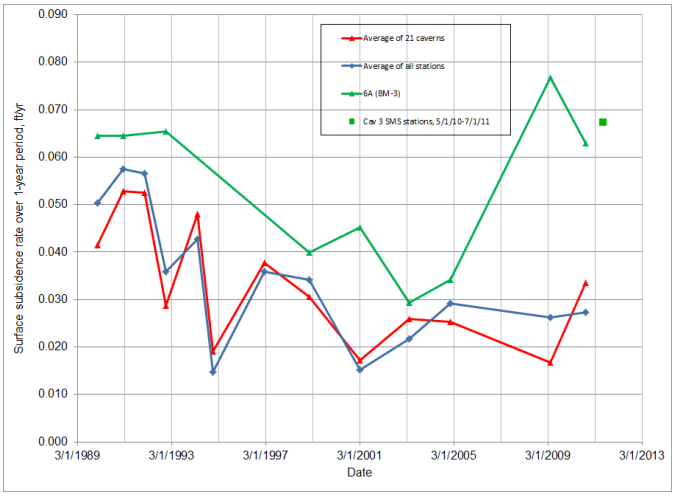

Fig. 15. Subsidence rates calculated between each site-wide data collection (in feet/year).

Finally, new simulations were performed to analyze the effect of the increased subsidence over Cavern 3. Because of the previous reports of leakage in Cavern 3, the new analyses assumed that brine pressure in a damaged Cavern 3 was slowly decreasing at a rate of 1.06 kPa/yr beginning in late 2003. (There are other potential causes of the increased subsidence, primarily involving voids in the overlying caprock, but they were not considered in this analysis.) A lower pressure in the cavern results in a greater difference between cavern and in situ pressures, thus increasing the creep rate. The exact mechanism which would cause such a pressure decrease is not known at this time (perhaps a preferential path through the borehole to the caprock, into which the brine can flow).

4. RESULTS

4.1. Damaged Caprock Model Results

The amount of output from these runs is quite voluminous, so only a small subset will be shown here, but the following conclusions can be drawn from the results obtained by these calculations:

- The calculations show that the irregular pattern of mining activities can potentially create stress conditions that exceed the collapse pressure of the steel casings, and the yield stresses of both the steel and cement.
- Potential damage conditions tend to occur more often near the top of the caprock, which correlates with observed damage.
- Conditions are also created for which a combination of elongation of the casings and shear or compressive stresses, though each alone is less than the damage threshold, may combine to create damage conditions.

Axial strain in caprock is strongly dependent on the modulus of the caprock in the immediate vicinity of the borehole. The higher strains occur over the caverns located below the weakened caprock. For the values of rock mass elastic modulus used in these calculations, the well strains did not exceed the damage thresholds over the hard salt; however, axial strains did exceed the 0.2-millistrain threshold over the soft salt. Figures 16 and 17 show the predicted axial strain in the caprock for the soft salt, and for either weakened caprock above cavern 2 (Fig. 16) or weakened caprock above caverns 1, 3, and 4 (Fig. 17). These demonstrate that well strain is a definite concern in mined areas of the dome in regions of soft salt. Furthermore, coupling the effects of axial strain with large compressive or shear stresses can lower the damage threshold for these boreholes. In all instances, the higher strains tend to occur near the top of the caprock.

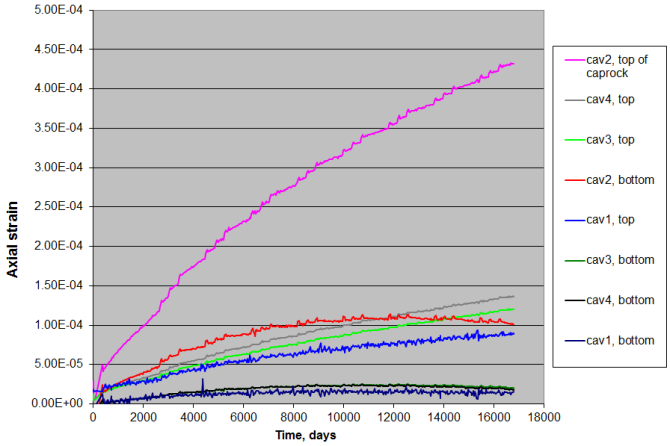

Fig. 16. Axial well strain in caprock, weakened caprock above cavern 2, in soft salt.

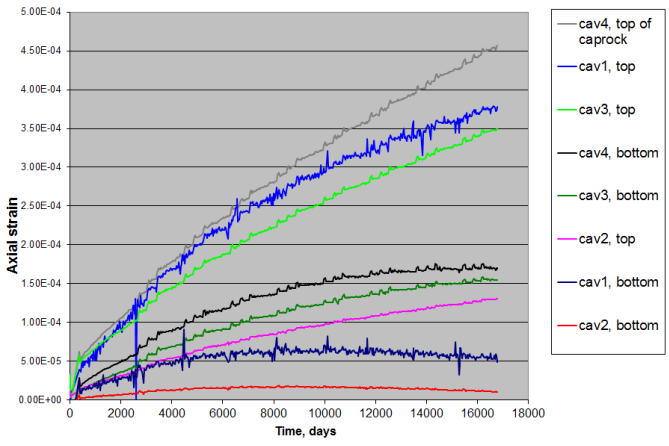

Fig. 17. Axial well strain in caprock, weakened caprock above caverns 1, 3, and 4, in soft salt.

Calculations of the maximum compressive stresses in the caprock show that well casings in areas that are not weakened by mining, but near other weakened areas, experience the highest values of compressive and bending stresses. Values of compressive stress are predicted to exceed the collapse pressure for the steel casings over soft salt in those circumstances. Similarly, predicted shear stresses in the caprock exceeded the threshold values for casings in undamaged caprock, but near regions of weakened caprock, and over the softer salt. The effect of weakening certain areas of the caprock creates conditions where greater stresses are distributed to non-weakened areas, causing potential wellbore damage conditions. The higher stresses were predicted to occur near the top of the caprock.

Based on the results described here, a priority list for well inspection was developed for Bryan Mound. Cavern 106 was recommended as the top priority; when it was inspected, significant shear damage to the casing was discovered in the top half of the caprock.

4.2. Cavern-Specific Creep Model Results

Table 4 lists the creep coefficients for both the 2009 [10] and the current analyses, showing the creep multiplier (the factor by which the creep coefficient A is multiplied) and a comparison between the predicted and measured cavern closure rate for each cavern under normal operating pressures. Cavern closure rates were matched very well for Caverns 101-102, 104-105, 107-108, 1-2, and 4-5. The closure rates for Caverns 114 and 115 are significantly higher than for all the other caverns, and their closure history is more difficult to match. Because of the close proximity of adjacent caverns, changing the creep multiplier on one cavern may affect the closure of a nearby cavern, making the process of developing good matches for all caverns highly iterative. The improved matches in closure rates resulted in much better matches of surface subsidence data. Figures 18 through 20 compare predicted and measured surface subsidence over the caverns, and these comparisons show a significant improvement over those in the 2009 analyses [10].

Table 4. Cavern-specific power law creep properties for Bryan Mound.

	Creep Multiplier		Cavern closure, normal pressure range, BBL/year		
Cavern	[10]	Current	Measured	[10]	Current
BM1	1.8	3.32	1,721	1,250	1,863
BM2	1.8	19.08	103	27	82
BM3	1.8	4.90	N/A	N/A	N/A
BM4	1.8	31.00	5,917	1,902	4,114
BM5	1.8	1.94	7,727	6,986	8,810
BM101	1.8	1.89	5,365	5,239	5,627
BM102	1.8	2.16	4,944	4,424	4,851
BM103	1.8	27.56	11,680	4,308	7,956
BM104	1.8	1.46	2,948	3,182	2,949
BM105	1.8	1.85	3,683	3,594	3,518
BM106	13	18.40	10,460	9,063	11,435
BM107	1.8	1.30	4,061	4,799	5,323
BM108	1.8	0.14	2,702	6,209	3,376
BM109	13	7.00	8,543	10,051	10,129
BM110	1.8	1.50	3,150	3,059	3,747
BM111	1.8	10.00	7,813	4,618	6,209
BM112	13	1.80	6,858	7,074	8,451
BM113	13	30.00	10,223	6,959	11,787
BM114	13	200.00	21,304	9,120	15,252
BM115	13	200.00	21,034	8,732	12,807
BM116	1.8	4.36	6,135	4,244	5,736
Hard Salt	1.8	2.3			
Soft Salt	13	24			

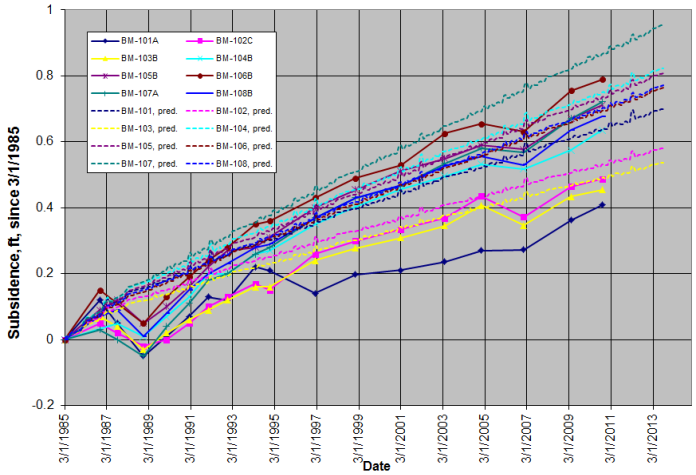

Fig. 18. Measured and predicted surface subsidence over Caverns 101-108, using cavern-specific creep properties.

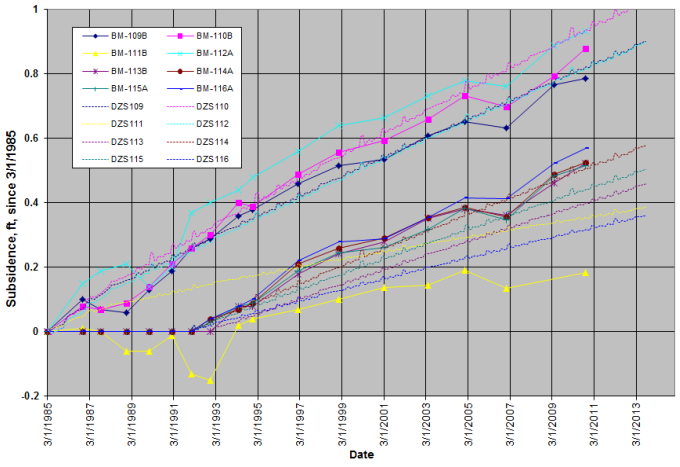

Fig. 19. Measured and predicted surface subsidence over Caverns 109-116, using cavern-specific creep properties.

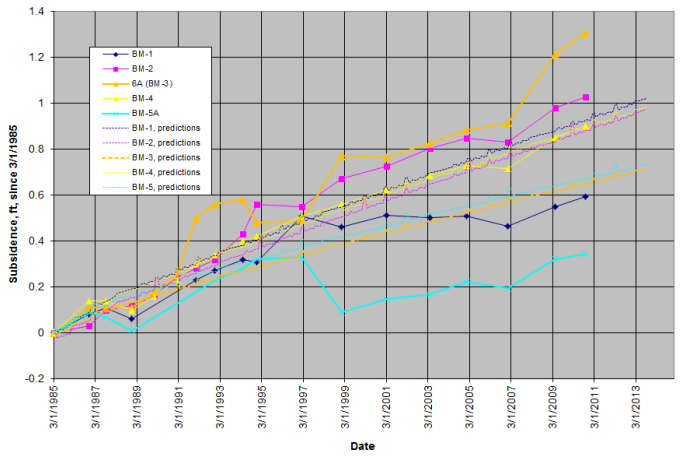

Fig. 20. Measured and predicted surface subsidence over Caverns 1-5, using cavern-specific creep properties.

4.3. Cavern 3 Model Results

Figure 21 presents two sets of contour plots of surface subsidence rate, one set for the case of an undamaged Cavern 3, the other for the damaged case. The contours for an undamaged Cavern 3 look like a typical bulls-eye centered over the middle of the cavern field. The contours for the damaged case, however, show the highest subsidence centered over Cavern 3, and resemble the plots shown in Figures 8 and 9 both in character and magnitudes. Therefore, the new simulations of a damaged Cavern 3 can be used to assess the potential effects of this enhanced subsidence.

One of the ways in which increased subsidence may impact the site is by putting overly high horizontal strains on surface structures. Figure 22 plots the minimum principal strains on the surface, at the times 12/1982, 8/2008, 4/2010, and 8/2013, for the scenario of a damaged Cavern 3. (Strains are assumed to be positive in tension, so for this case the most negative minimum strain corresponds to the maximum compressive strain.) The maximum compressive strains are predicted to occur over the eastern boundary of Cavern 3, with that strain predicted to approach the threshold of 1 millistrain by 2013 (at the middle of the region over Cavern 3) and exceed it by 2015. This value of 1 millistrain, in both tension and compression, is the accepted threshold value used in previous reports for identifying potential damage to surface structures. The greatest concern on the surface is the proximity of oil and brine storage tanks on the northern perimeter of Cavern 3 to the high-strain region. The storage tanks, along with their foundational structure and any nearby connecting equipment, are predicted to experience compressive strains in excess of 1 millistrain within the next 3-5 years. Maximum tensile strains are predicted to exceed 0.4 millistrains in tension on the west boundary of the salt dome, near the access road, within 3 years (i.e., the threshold value in tension is not predicted to be exceeded).

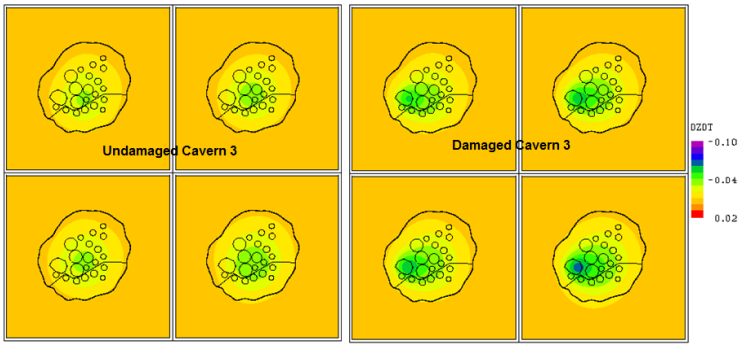

Fig. 21. Predicted subsidence rates (ft/yr), undamaged vs. damaged Cavern 3 (times August of 2010, 2011, 2012, 2013).

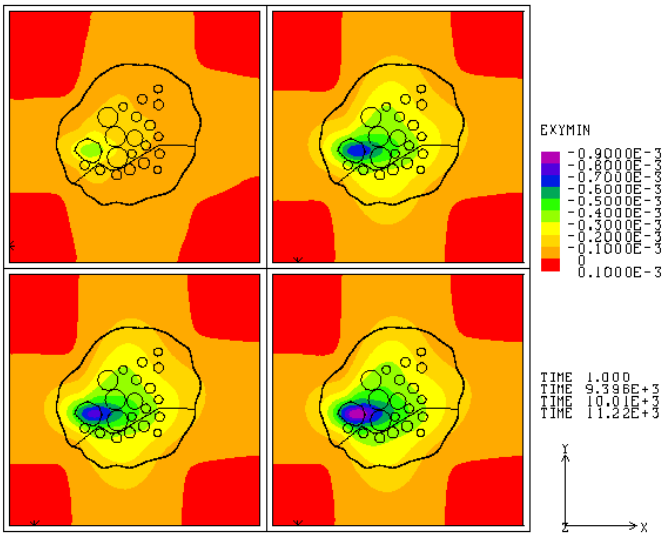

Fig. 22. Predicted minimum horizontal principal strains at the surface (12/1982, 8/2008, 4/2010, and 8/2013).

A second potential negative impact of a damaged Cavern 3 would be its effect on surrounding well casing structures. At well locations, subsidence will primarily induce elongation of the axis of the well. Under these conditions, the cemented annulus of the wells may crack forming a horizontal tensile fracture that may extend around the wellbore. This may not result in vertical fluid migration along the casing, but could permit horizontal infiltration into ground waters. Figure 23 plots the axial wellbore strain in salt for all the caverns. The precipitous change in the strain over Cavern 3 occurs when the simulation begins the pressure loss. Note the effect on the wellbore for Cavern 116, which is the cavern closest to Cavern 3. The strains on the casing reverse from tension to compression. This is due to the location of Cavern 3 near the top of the salt dome. The enhanced creep of Cavern 3 also affects the stresses in the salt around the wells for 116, increasing the shear stresses in that region. Even though the values of compressive strain and dilatant stresses around Well 116 do not exceed established thresholds for potential damage concern, the uncertainty in the changed stress environment is worthy of further investigation. Also, the

results in Figure 23 are obtained under the assumption that enhanced creep in Cavern 3 is the cause of the increased surface subsidence. Another potential cause of the subsidence may be collapse of void space in the caprock surrounding Well 3; three previous surveys of the wells at Cavern 3 noted the presence of a void in the caprock of several feet in height at around 818 feet depth.. If that or some other phenomenon is the cause of the increased subsidence, then the results in Figure 23 are not correct.

An additional observation to be made from Figure 23 is the extremely large tensile strains predicted for Caverns 114 and 115. These predictions are independent of anything involving Cavern 3, and are the result of the high cavern closure measured for those caverns. This figure would indicate that the well casing in the salt for Caverns 114 and 115 should be well into the plastic strain mode, and may be severely damaged; however, scoping measurements from those wells taken within the last year indicate only small trajectory misalignments and ovalities. Therefore, regarding the wellbores for Caverns 114 and 115, the predicted and actual states of the casings do not seem to agree.

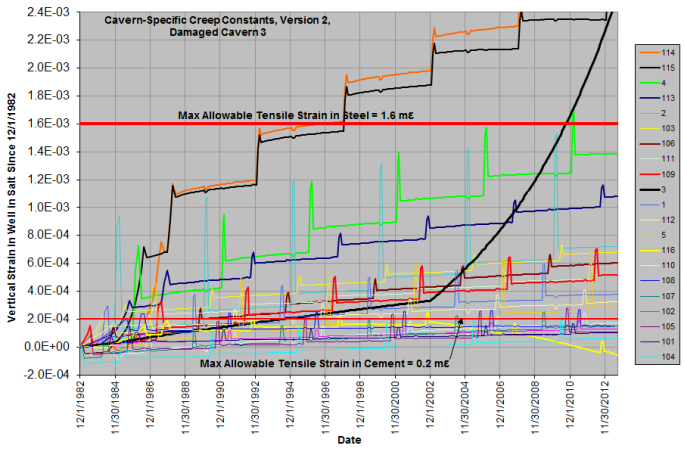

Fig. 23. Predicted axial wellbore strain in the salt, with a damaged Cavern 3.

5. CONCLUSIONS

The Bryan Mound site has been in operation for over 30 years, and the changes in stress in the cavern field have developed technical issues regarding the continued safe and efficient operation of the facility. These issues are compounded by highly heterogeneous geologic materials and abandoned caverns which contribute to the difficulty in understanding the current state of the underground structures. The analyses in this paper have produced the following conclusions:

- Boreholes located in weakened caprock, and over softer salt, are highly prone to tensile damage.
- Boreholes located in intact caprock, but near regions of weakened caprock, are more likely to experience collapse pressures and shear stresses that may damage the casings; this phenomenon has been observed in the field.
- The highly heterogeneous salt at Bryan Mound results in widely varying cavern closure rates, and makes development of a verifiable numerical model especially difficult.
- Surface subsidence measurements indicate that something has happened to or above Cavern 3 to increase subsidence, although there seems to be little if any effect on site-wide subsidence. Analyses indicate that surface facilities near the cavern could experience excessively high compressive strains in the next 3-5 years, if the model accurately depicts what is happening at the site.

There is a significant amount of uncertainty regarding the effect of the weakened caprock, highly heterogeneous salt, and the current state of Cavern 3 on surface and subsurface facilities at Bryan Mound. The types of uncertainty include the following:

- Scarcity of data/information – There is very little understanding of the areal extent of the damage to the caprock, and how that damage is manifested. Also, the only data currently being used to monitor Cavern 3 are from elevation data taken from the monuments.
- Analytical uncertainties – Two significant uncertainties in the computational analyses previously mentioned include the large amount of heterogeneity of the creep properties across the salt dome, and the non-uniform damage to the caprock due to sulfur mining. An additional uncertainty is the mechanism that is causing increased subsidence over Cavern 3. Whether caused by enhanced creep in the salt, or by collapsing caprock, or by some other mechanism, the cause will have a significant impact on the distribution of stress changes on surrounding structure.

6. ACKNOWLEDGEMENTS

Sandia National Laboratories is a multi-program laboratory managed and operated by Sandia Corporation, a wholly owned subsidiary of Lockheed Martin Corporation, for the U.S. Department of Energy's National Nuclear Security Administration under contract DE-AC04-94AL85000.

REFERENCES

1. Hogan, R. G., ed., 1980. *Strategic Petroleum Reserve (SPR) Geological Site Characterization Report: Bryan*

Mound Salt Dome, SAND80-7111. Sandia National Laboratories, Albuquerque, New Mexico, USA.

2. Preece, D.S. and Foley, J.T., 1984. *Long-Term Performance Predictions for Strategic Petroleum Reserve (SPR) Caverns*, SAND83-2343, Sandia National Laboratories, Albuquerque, New Mexico, USA.

3. Neal, J.T., Magorian, T.R., and Ahmad, S., 1994. *Strategic Petroleum Reserve (SPR) Additional Geologic Site Characterization Studies Bryan Mound Salt Dome, Texas*, SAND94-2331. Sandia National Laboratories, Albuquerque, New Mexico, USA.

4. Stein, J.S. and Rautman, C.A., 2005. *Conversion of the Bryan Mound Geological Site Characterization Reports to a Three-Dimensional Model*, SAND2005-2009, Sandia National Laboratories, Albuquerque, New Mexico, USA.

5. Rautman, C.A. and Snider Lord, A., 2007. *Sonar Atlas of Caverns Comprising the U.S. Strategic Petroleum Reserve Volume 3: Bryan Mound Site, Texas*, SAND2007-6067, Sandia National Laboratories, Albuquerque, New Mexico, USA.

6. Lord, A.S., 2007. "An Updated Three-Dimensional Site Characterization Model of the Bryan Mound Strategic Petroleum Reserve Site, Texas," Letter Report to W. Elias, DOE PMO, November 5, 2007.

7. Keplinger and Associates, 1980. "Report of Investigations on Cavern #3, Bryan Mound Strategic Petroleum Reserve, Freeport, Texas," for Dravo Utility Constructors Inc. and U.S. Department of Energy, New Orleans, Louisiana, August 30, 1980

8. Lord, A.S., 2009. "April 2009 Bryan Mound Subsidence Analysis," Letter Report to R. Myers, Strategic Petroleum Reserve, November 16, 2009.

9. Lord, A.S., 2010. "October 2010 Bryan Mound Subsidence Analysis," Letter Report to W. Elias, Strategic Petroleum Reserve, March 24, 2010.

10. Sobolik, S.R. and Ehgartner, B.L., 2009. *Analysis of Cavern Stability at the Bryan Mound SPR Site*, SAND2009-1986, Sandia National Laboratories, Albuquerque, New Mexico, USA.

11. Munson, D.E., 1998. *Analysis of Multistage and Other Creep Data for Domal Salts*, SAND98-2276, Sandia National Laboratories, Albuquerque, New Mexico, USA

12. Blanford, M.L., Heinstein, M.W., and Key, S.W., 2001. *JAS3D. A Multi-Strategy Iterative Code for Solid Mechanics Analysis. User's Instructions, Release 2.0*. SEACAS Library, JAS3D Manuals, Computational Solid Mechanics / Structural Dynamics, Sandia National Laboratories, Albuquerque, New Mexico

13. Morgan, H.S. and Krieg, R.D., 1990. *Investigation of an Empirical Creep Law for Rock Salt that Uses Reduced Elastic Moduli*, SAND89-2322C, presented at the 31st U.S. Symposium on Rock Mechanics held in the Colorado School of Mines in June 18-20, 1990.

14. Wawersik, W.R. and Zeuch, D.H., 1984. *Creep and Creep Modeling of Three Domal Salts – A Comprehensive Update*, SAND84-0568, Sandia National Laboratories, Albuquerque, New Mexico.

15. Sattler, A. and Sobolik, S.R., 2010. "Geomechanical Analysis of the Bryan Mound SPR Site with Mining-Induced Damage in the Caprock," letter report to R. Myers, DOE-SPR, August 12, 2010.

16. Park, B.Y., Herrick, C.G., Ehgartner, B.L., Lee, M.Y., and Sobolik, S.R., 2006. Numerical Simulation Evaluating the Structural Integrity of SPR Caverns in the Big Hill Salt Dome. In *Proceedings of the 41st U.S. Symposium on Rock Mechanics (USRMS): "50 Years of Rock Mechanics - Landmarks and Future Challenges,"* ARMA 06-924, Golden, Colorado, June 17-21, 2006.

17. Sobolik, S.R. and Ehgartner, B.L., 2012. *Analysis of the Stability of Cavern 3 at the Bryan Mound SPR Site*, SAND2012-TBD, under review, Sandia National Laboratories, Albuquerque, New Mexico, USA.